Temperature Distribution Simulation in an MV Switchgear Bus Bar Chamber

Mijodrag Miljanovic[1], Martin Kearns[2], Brian G Stewart[1]

[1]Department of Electronic and Electrical Engineering, University of Strathclyde, Glasgow, Scotland, UK

[2]EDF Energy, East Kilbride, Scotland, UK

***Abstract-* Temperature is one of the main contributors for the decrease of switchgear insulation withstand capability and life expectancy. Unattended temperature rise can lead to overheating of switchgear insulation causing insulation breakdown and hence switchgear outage. This work presents a simulation investigation of how temperature hot spots may be detected by studying the surface temperature distribution along a switchgear bus bar chamber wall. A three-dimensional (3-D) finite element method (FEM) MV switchgear bus bar chamber is created. The heat dissipation caused by bus bar load currents and thermal localized hot spots caused by increased contact resistances is investigated. It is shown that it may be possible to detect inner hot spots on the surface of switchgear chamber walls. It is also shown that the coating and the emissivity factor of the walls have a significant influence on the detected surface temperature.**

Keywords- switchgear insulation; temperature distribution, EM and thermal analysis; finite element method (FEM); bus bar

I. Introduction

The withstand capability of insulation within medium voltage (MV) switchgear depends on a large scale on localized temperature. Over-temperature is recognized as one of the main failures causes for insulation breakdown [1]. It is also reported that the detection of temperature hot spots in MV switchgear is one of the most important condition monitoring goals [2]. To ensure extended life time of MV equipment the electrical insulation has to be kept within permissible temperature limits which are defined by IEC 62271-202:2014 and IEEE C37.23-2015 standards. During regular operational periods the environmental conditions of switchgear changes. Vibration, contamination and other factors can cause the resistance of contact joints to increase which consequently leads to higher temperatures within a switchgear compartment. Therefore, it is important to take temperature measurements into key condition monitoring objectives.

There are many approaches used to monitor and to estimate temperature for different components within MV switchgear. Some of these approaches are defined by standards while others are based on component experiences. In the technical regulation for MV switchgear guidance PD CLC IEC/TR 62271-307:2019, it is highlighted that temperature rise calculations within MV switchgear can be evaluated according to low voltage (LV) assembly technical report IEC/TR 60890. In [3] an approach for the estimation of the temperature rise of circuit breaker contacts based on that report within an air insulated MV switchgear is conducted. It is also known that in LV cabinets a uniform heat distribution is considered whereas this is not the case in MV switchgear. In [4] this problem is addressed with the conclusion that the temperature distribution factor needs to be adjusted when applying this regulation on MV switchgear.

In [5] a solution is presented on how to monitor and predict the temperature of “live” parts in a MV switchgear. In [6] infrared (IR) temperature sensors are applied to measure the temperature in MV switchgear through the application of an IR window. In [7] high temperature developments in bus bars have been investigated and some measures proposed on how to reduce temperature during the construction design.

Almost all of the investigations above attach temperature sensors on live parts for condition monitoring or require constructional changes to switchgear. However, for the attachment of temperature sensors on live parts the system needs to be taken out of service and safety precautions require to be undertaken. These actions are time-consuming and cost intensive processes. For the case of extended MV switchgear line up assemblies, there is also the need to estimate temperature without power cut-off and opening up of the equipment.

Based on the above, the aim of this study is to investigate the possibility of monitoring the temperature within MV switchgear bus bar compartments through simulating and understanding the outer surface temperatures of a bus bar compartment. Such an investigation may permit the attachment of surface temperature sensors to detect critical inner temperature levels. The advantage would be that there is no need for switching off the system.

The paper is structured as follows. In section II the creation of the simulation model is explained. In section III results are presented and in section IV conclusions are drawn.

II. Simulation Model

A bus bar compartment from an arbitrary switchgear is used as an example to build up a simulation model, as shown in Fig. 1. Finite element method (FEM) simulation using Comsol Multiphysics software is applied. In the first stage of the development, single parts of the compartment are created using the geometry feature in Comsol. These parts are then attached to an entire bus bar compartment. Afterwards, the bus bar compartment model is imported into the simulation environment and the materials assigned. The bus bar compartment is comprised of double bus bar conductors for

This is a peer-reviewed, accepted author manuscript of the following paper: Miljanovic, M., Kearns, M., & Stewart, B. G. (2022). Temperature distribution simulation in an MV switchgear bus bar chamber. 1-4. Paper presented at 2022 IEEE Conference on Electrical Insulation and Dielectric Phenomena, Denver, Colorado, United States.

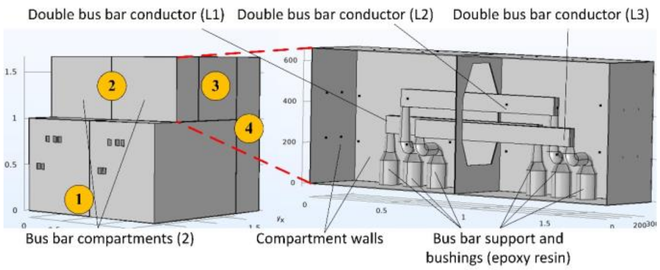

Fig. 1. Switchgear and bus bar compartment model: (1) Circuit breaker; (2) Bus bar compartment; (3): Current transformer; (4): Cable compartment.

each phase which are made from copper with a cross section of 10 x 85 mm². The sidewalls are made from steel with a thickness of 3 mm. The bushings and supports are made from epoxy resin. The simulation is setup through the application of three different so-called Comsol features. These are the Electric Circuit, the Electrical Currents and the Heat Transfer in Solids and Fluids features, which are coupled together by a Multiphysics node.

The Electric Currents feature is applied to define the 3-phase circuit, which is shown in Fig. 2. A 50 Hz AC voltage (U_s) of 12 kV rms in each phase is applied to drive the load currents (I_L). A load resistance (R_L) of 4.8 Ω is used to achieve a rated current of 2500 A for the bus bar conductors. The red dots in the circuit in Fig. 2 specify the circuit nodes which are also used to interconnect the circuit with the bus bar conductors in the Electrical Currents feature. The Electric Currents feature is used to define physical properties of the bus bars and contact resistances that are heated due to the conduction of currents. Circuit nodes 1 to 3 and 4 to 5 in Fig. 2 are used to interconnect the voltage source and the load resistance with the bus bar conductors, see Fig (3). The load currents are given by (1).

$$I_L = \frac{U_S}{R_L} \qquad (1)$$

The Heat Transfer feature is applied to simulate the heat distribution generated by the bus bars within the compartment and along the chamber surfaces. Throughout a Multiphysics feature, the calculated cycle losses from the electric current is coupled with the Heat Transfer feature. Whereas electric currents are implemented in the frequency domain to estimate the cycle average resistive losses, heat transfer is implemented in the time domain. The effect of the resistive heating of currents could also have been conducted in the time domain. The advantage of the frequency domain is that the calculation time is reduced considerably. The simulation is performed to investigate the influence of phase contact resistance increases on temperature changes at the compartment surface.

In the model, the heat dissipation by bus bars (R_{BB}) and increased contact resistance (R_{CT}) is considered in the form of conduction, natural convection and radiation, according to (2).

$$(R_{BB} + R_{CT}) * I_L^2 = P_{cond} + P_{conv} + P_{rad} \qquad (2)$$

The conduction part is directly transferred to the parts which are connected to the bus bars.

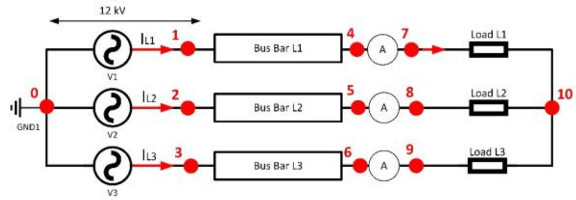

Fig. 2. 3-Phase circuit implemented to drive currents through bus bars in Electrical Circuit feature.

On the other hand, the enclosure absorbs the dissipated heat from convection and radiation. The absorbed heat by the enclosure is further transferred to the surrounding environment, where an air sphere is applied to enable the heat transfer. To measure the temperature, Comsol probes are attached on the compartment surfaces on the front, side and top walls of the chamber as indicated in Fig. 3. In addition, Comsol probes are also attached on the phase contacts that are going to be the source of localized resistive thermal heating in the investigation.

III. Simulation Results

A. Introduction

Simulations are carried out with an ambient temperature of 20 °C. The identification of potential hot spots is investigated by the application of increased contact resistances at contacts where the bus bar is connected to the conductor coming through bushings, see Fig. 3. At these spots, electrical contacts are applied to be able to increase the transition resistance. An ordinary contact resistance is implemented according to [8] with a value of 5 µΩ. The applied increased contact resistances in this study will be ten times the value of the ordinary contact resistance to model a degraded joint contact problem.

A. Rated Load without Increased Contact Resistance

The first simulation was carried out with rated current of 2500 A without any increased contact resistance. The simulation of the temperature is performed for a period of 500 min when temperature equilibrium is reached. In Fig. 4(a) the temperature profile of the compartment is shown from the front side view. Over the entire compartment a more or less even temperature distribution is established. In Fig. 4(b), the temperature profile of the bus bar conductors is shown. It can be seen that an even temperature distribution along the bus bars is produced since there is no localized contact resistance. In Fig. 4(c) the temperature development at the compartment surface is shown.

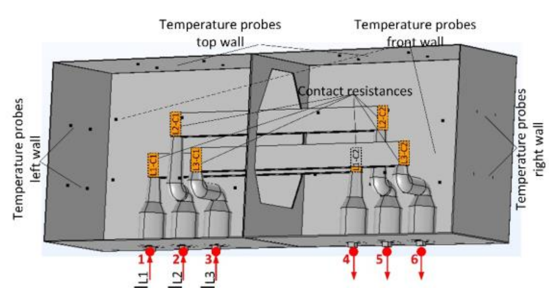

Fig. 3. Interconnection of bus bars to Electrical Current feature and position of probes and contact resistances.

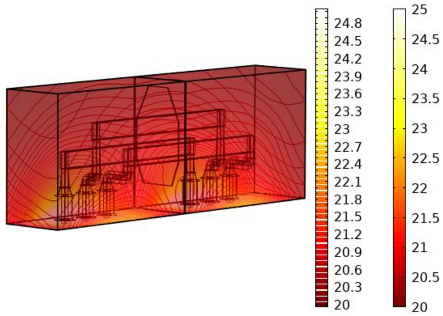

(a) Temperature profile of chamber surface

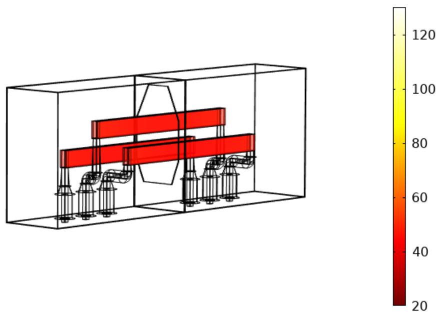

(b) Temperature profile of bus bar conductors

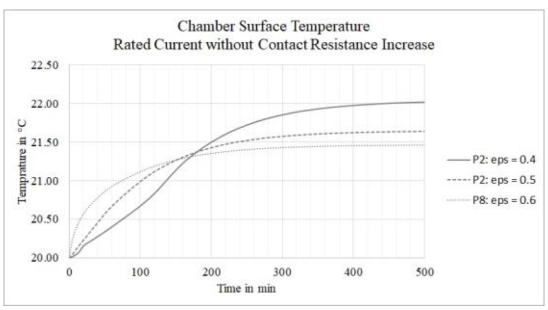

(c) Temperature along the surface

Fig. 4. Rated load without increased contact resistance.

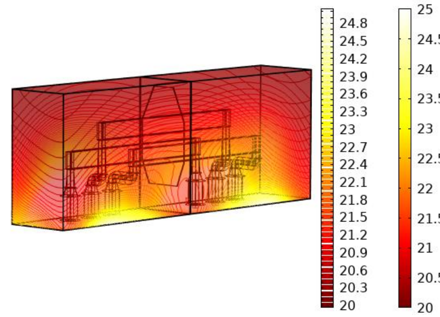

(a) Temperature profile of chamber surface

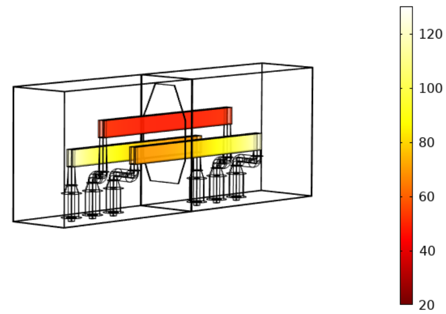

(b) Temperature profile of bus bar conductors

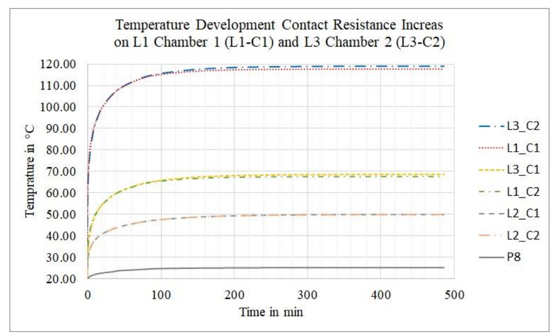

(c) Temperature development

Fig. 5. Increased resistance on L1 in chamber 1 (L1-C1) and L3 in chamber 2 (L3-C2).

Depending on the surface coating and consequently on the surface emissivity factor, the temperature of the surface varies. For the case of different emissivity factors of 0.4 and 0.5 the highest temperature occurs at probe 2 (P2). In contrast, for the case of an emissivity factor of 0.6 the highest temperature occurs at probe P8. It can also be seen that the higher the emissivity, the lower the temperature at the compartment surface. Therefore, it can be concluded that the detected temperatures along the compartment surface depends highly on the coating of the structure. For the following simulations, the emissivity factor is set to be 0.6.

B. Increased Contact Resistance on L1 Chamber 1 and L3 Chamber 2

In the following simulation the contact resistance on phase L1 in chamber 1 (L1-C1) was increased to ten times the ordinary value, i.e. to 50 μΩ. The same was implemented for the contact on phase L3 in chamber 2 (L3-C2). In Fig. 5(a) the temperature profile of the compartment is shown after temperature equilibrium was established. Compared to the case without additional contact resistance, an clear uneven temperature distribution along the entire compartment is evident. The lower part of the compartment has a slightly higher surface temperature compared to the top half. This might be a consequence of the affected bus bars positioned more in the lower part of the chamber and and always having a high temperature. In Fig. 5(b) the temperature distribution along the bus bar conductors is shown. Comparing the profile to Fig. 4(b) with ordinary contact resistance, an uneven temperature profile exists along conductors L1 and L3 due to the increased heating of the contact resistance. In Fig. 5(c) the temperature development of the contacts and surface probe P8 is shown - the highest surface temperature reached is around 25 °C. From the graphs, the temperature of contact L1 in chamber 1 (L1-C1) and L3 in chamber 2 (L3-C2) have similar values around 119 °C. The graphs also show a temperature increase on contacts L3-C1 and L1-C2 due to heat conduction through the bus bar conductors. It is noted that the temperature profiles on the surface top and surface side walls do not show any significant increase compared to the temperature profile on the front wall.

C. Increased Contact Resistance on L2 Chamber 1 and L2 Chamber 2

The contact resistance was increased on phase L2 and phase L3 in compartment 2, and are raised again to 50 μΩ. In Fig. 6(a) the surface temperature of the compartment is shown. Comparing with the temperature distribution in Fig. 5(a), a slight difference in the temperature distribution can be recognized at the right bottom side of the compartment. This is due to the fact that both heat sources are positioned in compartment 2. In Fig. 6(b) a higher temperature distribution along bus bar conductors L2 and L3 compared to bus bar L1 is clearly visible. Since bus bar conductor L1 is not affected by any resistance increase, its temperature level remains mainly unaffected and does not accumulate significant heat transfer from other sources.

In Fig. 6(c) the temperature development of the contacts is displayed. The contact temperature of L2-C2 and L3-C2 is around 120 °C due to the higher resistance.

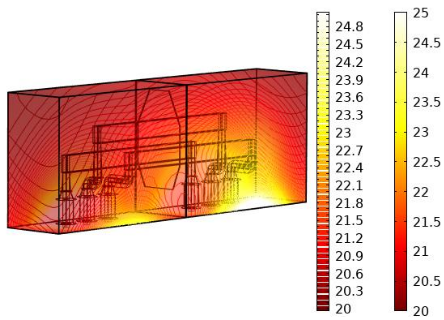

(a) Temperature profile of the bus bar compartment surface

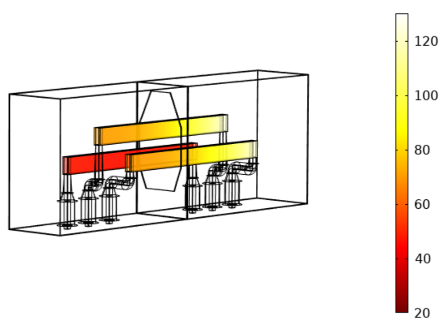

(b) Temperature profile of bus bar conductors

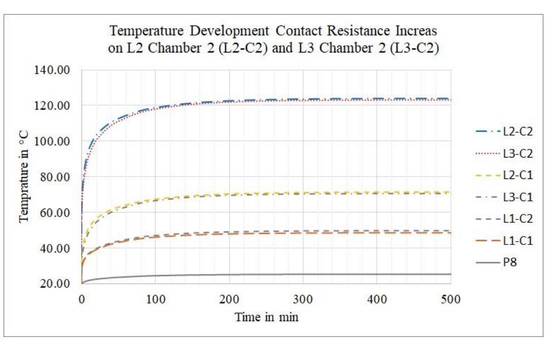

(c) Temperature development

Fig. 6. Increased contact resistance on L2 in chamber 2 (L2-C2) and L3 in chamber 2 (L3-C2).

The contacts in compartment 1, L2-C1 and L3-C1, are also affected due to heat conductivity from the bus bar. Their temperatures increase also by around 20°C compared to the regular load conditions. The highest measured temperature on the compartment surface was detected by probe P8 with a value of 25 °C. Interestingly, in this case, the highest temperature occurs again on the surface of the front wall.

IV. CONCLUSIONS

Surface temperature profiles were simulated for a switchgear chamber under load conditions with no localized bus bar connection contact problem. It was also shown that surface temperature levels depend highly on coating and emissivity factors. For the case of the occurrence of hot spots within the bus bar compartment, due to increased contact resistance, the surface temperature profiles within the compartment change from a presumed normal operational situation. Depending on the position of the heat source, the temperature profile internally and on the compartment surfaces change. As a consequence, these changes may be useful to detect potential internal hot spots. Interestingly, the highest temperature measured by the Comsol probes is on the front wall of the compartment potentially making this surface useful for passive temperature monitoring. Further studies will be undertaken to estimate optimal positions of temperature sensors to enable efficient switchgear temperature condition monitoring.

ACKNOWLEDGMENT

This work was funded by the EDF (UK).

REFERENCES

[1] Z. Linsuo and W. Maojun, *The Design and Realization of on-line Measuring Device of Busbar Temperature Rise for HV Switch Board*, 2006 International Conference on Power System Technology, 2006, pp. 1-5CIGRE/CIRED, August 2018.

[2] ABB, *Switchgear temperature monitoring – Early hot spot detection enabling condition-based maintenance*, White paper, ABB, July, 2016.

[3] E. Fjeld, W. G. J. Rondeel, E. Attar and S. Singh, *Estimate the Temperature Rise of Medium Voltage Metal Enclosed Switchgear by Simplified Heat Transfer Calculations*, in *IEEE Transactions on Power Delivery*, vol. 36, no. 2, pp. 853-860, April 2021.

[4] E. Fjeld, W. Rondeel, K. Vaagsaether, E. Attar, *Influence of heat source location on air temperatures in sealded MV switchgears*, 24th International Conference & Exhibition on Electricity Distribution (CIRED), Volume 2017, Issue 1, 2017 , p. 233 - 237 IET Journals, 2018.

[5] J. Li, Y. Sun, N. Dong and Z. Zhao, *A Novel Contact Temperature Calculation Algorithm in Distribution Switchgears for Condition Assessment*, ," in *IEEE Transactions on Components, Packaging and Manufacturing Technology*, vol. 9, no. 2, pp. 279-287, Feb. 2019.

[6] L. Zhiwei, Z. Kehui and Z. Xiaochun, *Research on Fault Diagnosis of Switchgear Contacts Based on BP Neural Network*, 2018 International Conference on Power System Technology (POWERCON), 2018, pp. 3507-3513.

[7] J. Lotiya*, Thermal analysis and optimization of temperature rise in busbar joints configuration by FEM*, 2014 6th IEEE Power India International Conference (PIICON), 2014, pp. 1-5.

[8] S. W. Park and H, *A practical study on electrical contact resistance and temperature rise at at the connections of the copper busbars in switchgears*, 2014 IEEE 60th Holm Conference on Electrical Contacts (Holm), 2014, pp. 1-7.